arXiv:0902.2602v2 [astro-ph.SR] 17 Feb 2009

CHARA/MIRC interferometry of red supergiants: diameters, effective temperatures and surface features

L.L. Kiss[1], J.D. Monnier[2], T.R. Bedding[1], P. Tuthill[1], M. Zhao[2], M.J. Ireland[1], T.A. ten Brummelaar[3]

Abstract.
We have obtained *H*-band interferometric observations of three galactic red supergiant stars using the MIRC instrument on the CHARA array. The targets include AZ Cyg, a field RSG and two members of the Per OB1 association, RS Per and T Per. We find evidence of departures from circular symmetry in all cases, which can be modelled with the presence of hotspots. This is the first detection of these features in the *H*-band. The measured mean diameters and the spectral energy distributions were combined to determine effective temperatures. The results give further support to the recently derived hotter temperature scale of red supergiant stars by Levesque et al. (2005), which has been evoked to reconcile the empirically determined physical parameters and stellar evolutionary theories. We see a possible correlation between spottedness and mid-IR emission of the circumstellar dust, suggesting a connection between mass-loss and the mechanism that generates the spots.

1. Introduction

Red supergiants (RSGs) represent an important but still poorly characterized evolutionary phase of massive stars. They are key agents of nucleosynthesis and chemical evolution of the Galaxy, and have also long been known for their slow optical variations. This variability is usually attributed to radial pulsations, although irregular variability caused by huge convection cells was also suggested from theory (Schwarzschild 1975) and observations of hotspots on late-type supergiants (Tuthill et al. 1997). From the most extensive study of RSG variability to date, Kiss et al. (2006) found a strong $1/f$ noise component in the fluctuations of 48 bright galactic objects, a behaviour that fits the picture of irregular photometric variability caused by large convection cells, analogous to the granulation background seen in the Sun. In addition, a significant fraction of the sample shows two distinct time-scales of variability, where the slower one resembles the enigmatic Long Secondary Periods (LSPs) of the less massive and luminous Asymptotic Giant Branch stars (Wood et al. 2004).

The best-studied individual RSG in terms of multi-wavelength surface imaging is the nearest one, Betelgeuse, which has long been known to show a ∼400 d

[1]Sydney Institute for Astrophysics, School of Physics, University of Sydney, NSW 2006, Australia

[2]Department of Astronomy, University of Michigan at Ann Arbour, Ann Arbour, MI 48109-1090

[3]The CHARA Array, Georgia State University

pulsation period and a $\sim$2000 d LSP. For this star, a decade of interferometric hotspot observations has revealed an irregular shape of the stellar image, the possible imprint of giant convection cells that were confirmed qualitatively with 3D stellar convection models (Freytag et al. 2002). Young et al. (2000) found a strong variation in the apparent asymmetry as a function of wavelength, with a featureless symmetric disk at 1.290 μm that is in stark contrast with the presence of hotspots in the optical range. This has led to the suggestion that the bright spots are unobscured regions of elevated temperature seen through a geometrically-extended and line-blanketed atmosphere, in which the features are seen along lines of sight for which the atmospheric opacity has been reduced as the result of activity, such as convection, at the stellar surface (Young et al. 2000). Extending these results to the H-band at 1.6 μm, where an opacity minimum in the cool atmospheres permits seeing through very close to the photosphere, one would expect negligible or no evidence of hotspots at this band.

Inspired by the open questions in regards of surface structures of RSGs (e.g.: What is the physical mechanism that creates the hotspots? How is the spottedness related to the fundamental stellar parameters and the presence of LSPs?), we performed a single-epoch mini-survey of several RSGs using the CHARA interferometric array.

2.   Observations and target selection

Our observations were carried out on six nights in July-August 2007 at the Georgia State University Center for High Angular Resolution Astronomy (CHARA) interferometer array using the Michigan Infra-Red Combiner (MIRC). The CHARA array, located on Mount Wilson, consists of six 1 m telescopes. It has 15 baselines ranging from 34 m to 331 m, providing resolutions up to $\sim$0.5 mas at H-band (ten Brummelaar et al. 2005).

The MIRC instrument was used to combine four CHARA telescopes, providing six visibilities, four closure phases, and four triple amplitudes simultaneously in eight narrow spectral bands (Monnier et al. 2006). Using the same W1-W2-S2-E2 configuration of CHARA that was used for surface imaging of Altair (Monnier et al. 2007), we achieved excellent (u, v) coverage of each tar-
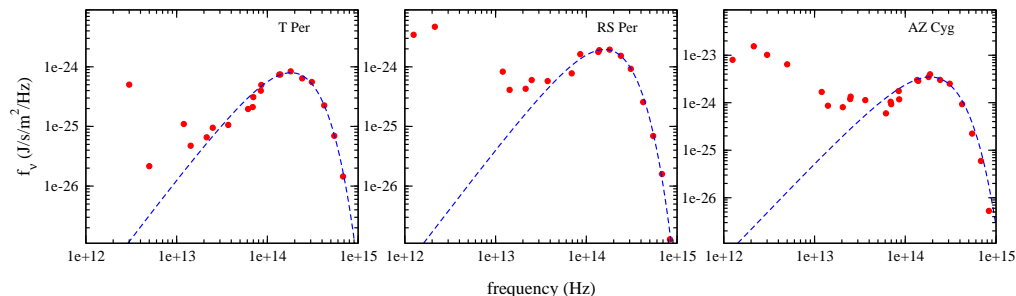

Figure 1.   Spectral energy distributions of the three observed RSGs. The dashed lines show blackbody fits to the optical–near-IR parts of the spectra, unaffected by the circumstellar emission at longer wavelengths.
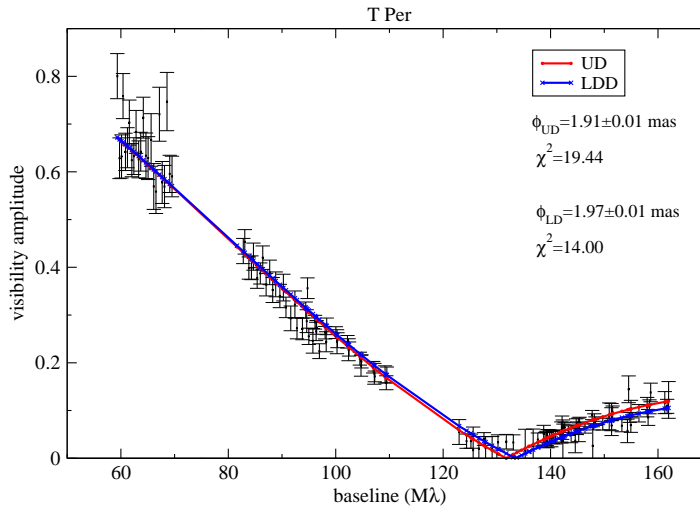
Figure 2. Visibility fits for T Per using uniform and limb-darkened disk models. The large χ^2 values reflect the simple models' inability to fit the triple amplitudes and the non-zero closure phases, which indicate significant departures from point symmetry.

get. The longest baseline in this configuration is 251.3 m, corresponding to a resolution of 0.68 mas at 1.6μm. We observed our targets along with one, two or three calibrators on each night, depending on the sky conditions. The data were reduced by the pipeline outlined by Monnier et al. (2007) and then combined by observing blocks and nights.

The initial list of targets contained several stars in the Per OB1 association and the galactic field. Of these, we collected data for RS Per, T Per, and AZ Cygni. Note that RS Per is a firmly established member of NGC 884 (d=2.34±0.05 kpc, Slesnick et al. 2002), while T Per lies about 2 degrees away in the outskirt of the Perseus "double cluster". AZ Cyg, located in the galactic plane (b=0.52), is not known to be a member of a young association; in addition to the 495 d pulsation period, it has a ~9-yr LSP (Kiss et al. 2006).

3. Results

We have employed different techniques to extract information from the interferometric data. Simple models were fitted using the latest modification of the MFIT[1] code by J. Young, originally written by M. Worsley. These included uniform and limb-darkened disks, elliptical disks and up to two hotspots. A Hestroffer-type power-law limb darkening with α=0.258 (Lacour et al. 2008) gave remarkably good fits of the visibilities in most cases. However, the simplest point-symmetric models fail for each of the three stars in closure phases and triple-amplitudes, which leaves no doubt about the detection of asymmetries in all three stars. We

---

[1] http://www.mrao.cam.ac.uk/~jsy1001/mfit/

have also obtained preliminary imaging using the MACIM code (Ireland et al. 2006).

3.1. Diameters and effective temperatures

We have determined the effective temperatures from the limb-darkened angular diameter:

$$T_{\text{eff}} = 7400 \left(\frac{F_{\text{bol}}}{10^{-13} \ \text{Wcm}^{-2}} \right)^{1/4} \left(\frac{1 \ \text{mas}}{\phi_{\text{LD}}} \right)^{1/2} \ \text{K}$$

(Perrin et al. 2004). The bolometric flux F_{bol} was computed by integrating a Planckian fit of the spectral energy distributions (SEDs), reconstructed from visual ($UBVRI$) and infrared data ($JHKLM$ + mid- and far-IR fluxes from IRAS, COBE and ISO) taken from various catalogues available through the Vizier service of the CDS, Strasbourg. The full SEDs (Fig. 1) clearly show circumstellar emission in the mid- and far-IR, so that blackbody fits were restricted to the unaffected shorter-wavelength part of the spectra ($<5 \ \mu$m).
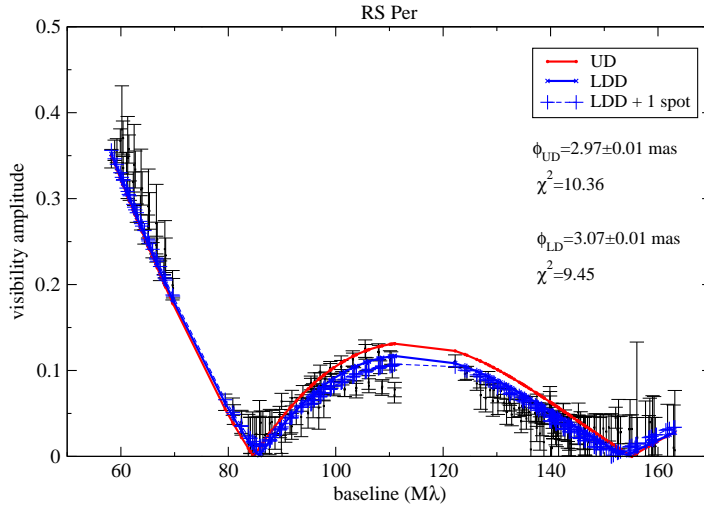

Figure 3.   Visibility fits for RS Per using uniform and limb-darkened disk models. Adding one hotspot improves the fit to $\chi^2 = 4.55$ without changing the size of the limb-darkened disk.

For T Per and RS Per, visibility data can be very well fitted with simple models. These are shown in Figs. 2-3. The dereddened fluxes and the LD disk diameters result in the following effective temperatures: T Per $- T_{\text{eff}} = 3670 \pm 117$ K; RS Per $- T_{\text{eff}} = 3551 \pm 71$ K, where the uncertainties are dominated by the uncertainties in interstellar reddening.

The significance of these temperatures is illustrated in Fig. 4, where we compare three RSG effective temperature scales. The excellent agreement between our data and the hotter temperature scale of Levesque et al. (2005) gives an independent confirmation of the new calibration, which was very successful in reconciling evolutionary models and observational properties of red supergiants.
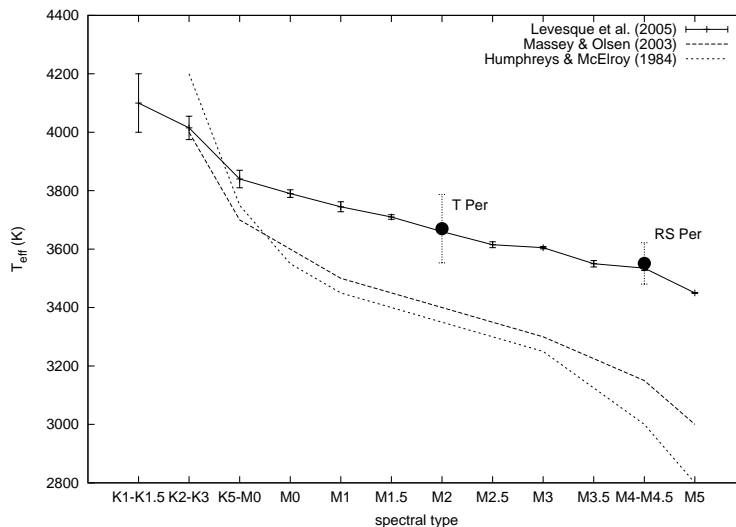
Figure 4.   Effective temperatures for T Per and RS Per, compared to three temperatures scales from the literature. Our results confirm the hotter scale of Levesque et al. (2005).

3.2.   Asymmetries, hotspots

We see evidence for hotspots with $\sim$10% flux contribution in all three stars, implying that: *(i)* hotspots are indeed ubiquitous in red supergiants; and *(ii)* these structures are visible in *H*-band too, in contrast to the Young et al. (2000) results for Betelgeuse at 1.29 μm. Considering the opacity minimum at 1.6 μm, these hotspots must be generated very close to the photosphere and their enhanced contrast can hardly be explained by opacity effects. Furthermore, in our admittedly small sample, the complexity of the observed stars seems to increase with the strength of circumstellar IR emission, which may indicate a connection between the hotspots and mass loss.

The most complex structures have been revealed for AZ Cyg, where the data suggest a brightness distribution almost like a contact binary with a $\sim$10-20% bright feature at the NW edge of the disk. Simple LDD + 1 spot models (Fig. 5) are roughly consistent with MACIM fits, but the analysis of this star is still in progress.

References

Freytag, B., Steffen, M., Dorch, B., 2002, AN, 323, 213
Humphreys, R.M., McElroy, D.B., 1984, ApJ, 284, 565
Ireland, M.J., Monnier, J.D., Thureau, N., 2006, Proc. SPIE, 6268E, 62681T
Kiss, L.L., Szabó, M.Gy., Bedding, T.R., 2006, MNRAS, 372, 1721
Lacour, S., et al., 2008, A&A, 485, 561
Levesque, E.M., et al., 2005, ApJ, 628, 973
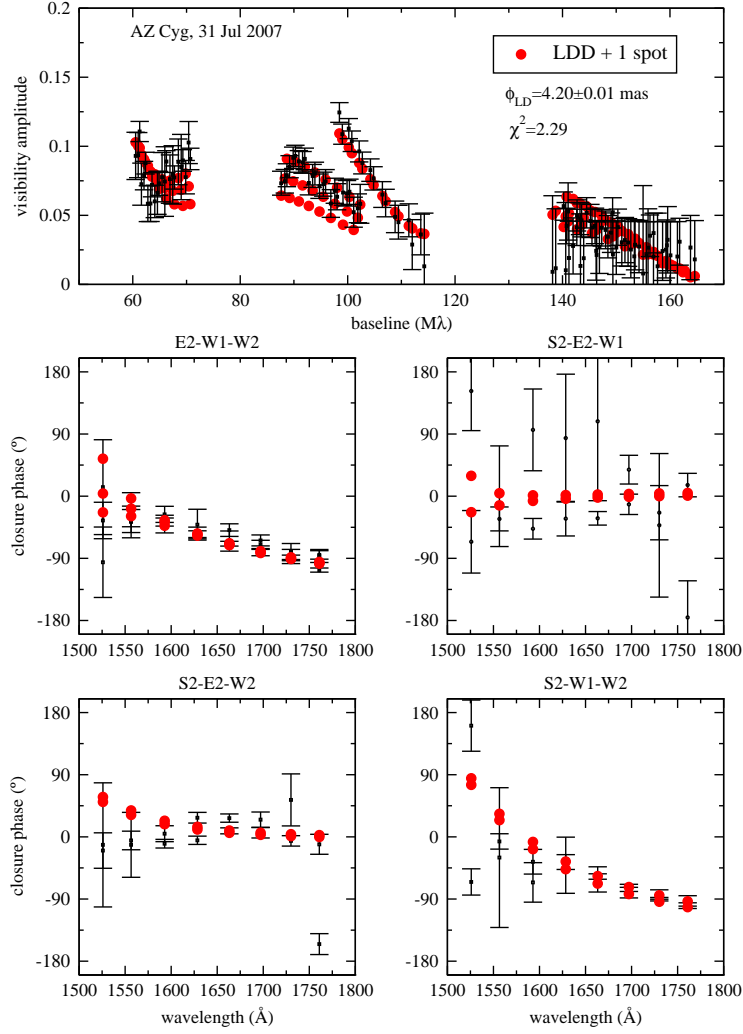
Figure 5.   Visibilities and closure phases for AZ Cyg on 31 July, 2007.

Massey, P., Olsen, K.A.G., 2003, AJ, 126, 2867

Monnier, J.D., et al., 2006, Proc. SPIE, 6268, 62681P

Monnier, J.D., et al., 2007, Science, 317, 342

Perrin, G., et al., 2004, A&A, 418, 675

Schwarzschild, M., 1975, ApJ, 195, 137

Slesnick, C., Hillenbrand, L.A., Massey, P., 2002, ApJ, 576, 880

ten Brummelaar, T.A., et al., 2005, ApJ, 628, 453

Tuthill, P.G., Haniff, C.A., Baldwin, J.E., 1997, MNRAS, 285, 529

Wood, P.R., et al., 2004, ApJ, 604, 800

Young, J.S., 2000, MNRAS, 315, 635